Revista Mexicana de Ciencias Geológicas, volumen 17, número 1
2000, p. 34-44
Universidad Nacional Autónoma de México, Instituto de Geología,
México, D.F.

AN ARC ANKARAMITE OCCURRENCE IN CENTRAL MEXICO

Luis Enrique Ortiz Hernández [1-2]

ABSTRACT

Melanocratic clinopyroxene-rich dikes intruding ultramafic cumulate rocks at the base of the Guanajuato magmatic sequence, in central Mexico, are classified as ankaramites.

They are high Mg, Cr and Ni basic rocks that have slightly enriched LREE-patterns, and Epsilon Nd (T=110 Ma) = +7.22 , which is consistent with their derivation from a high-field strength elements (HFSE) depleted source, within an island-arc setting. These magnesian rocks may have been parental to the mature tholeiitic and calc-alkaline series of this segment of the Guerrero terrane.

Key words: Ankaramite, dikes, arc magmatism, Guanajuato, central Mexico

RESUMEN

Los diques melanocráticos ricos en cristales de clinopiroxeno que intrusionan a rocas ultramáficas cumulíticas de la base de la secuencia magmática de Guanajuato son clasificados como ankaramitas. Estas rocas tienen altos valores de MgO, Cr y Ni, están ligeramente enriquecidas en tierras raras ligeras y un valor del Epsilon Nd (T=110 m a) = +7.22, lo que es congruente con su origen a partir de una fuente mantélica empobrecida en elementos con fuerte carga iónica (HFSE), en un contexto de arco magmático. Estas rocas magnesianas pueden ser el magma madre de las series toleítica madura y calcialcalina para este segmento del terreno Guerrero.

Palabras clave: Ankaramita, diques, magmatismo de arco, Guanajuato, México central.

INTRODUCTION

After the IUGS definition (Le Maitre et al., 1989), ankaramite is a porphyritic melanocratic basanite with abundant phenocrysts of pyroxene and olivine. These rocks were firstly defined by Lacroix (1916), in their type locality of Ankaramy, at Ampasindava, Madagascar.

Ocurrences of ankaramitic rocks and picrites have been reported in island arc settings in recent years (Bardsell and Berry, 1990; Foden, 1983; Ramsay et al., 1984).

Bardsell and Berry (1990) proposed the terms arc ankaramites and arc picrites for primitive, clinopyroxene or olivine phenocryst-rich, basaltic arc rocks, independent of their degree of SiO_2 saturation and alkali content. I have adopted the Bardsell and Berry definition for to the mafic, clinopyroxene-rich dikes intruding the ultramafic cumulates at the base of the Guanajuato magmatic sequence, exposed in central Mexico.

Field relationships, petrographic and geochemical data of these high-magnesium rocks are presented here, in order to correlate them with the magmatic evolution of this segment of the Guerrero terrane.

ANALYTICAL METHODS

Chemical analyses of ferromagnesian minerals, plagioclase, spinels and secondary minerals of the ankaramitic dikes were performed with a CAMEBAX automatized electron microprobe at the Grenoble University, France, with natural and synthetic mineral standards. Only analyses of the primary minerals are reported. Instrument operating conditions were 15 kV accelerating voltage, 10 nA beam current and 6 seconds counting time.

Core and rim analyses were made to check for zoning and overall homogeneity. Underthese analytical conditions concentrations less than 0.2 wt% are not considered as representative. Raw data were corrected by the on-line ZAF correction program of CAMEBAX (Hénoc and Tong, 1978). Structural formulae presented in Tables 2 and 3 were calculated by stoichiometry to 8 oxygens for the plagioclases, 32 oxygens for the spinels, 6 oxygens for the clinopyroxenes, and 23 oxygens (anhydrous) for the case of the amphiboles, according to the method described by Robinson and

[1] Consejo de Recursos Minerales, Gerencia de Investigación Aplicada. Blv. Felipe Angeles s/n km 93.5 Col. Venta Prieta, C.P. 42080 Pachuca, Hgo.
[2] Instituto Politécnico Nacional, Sección de Estudios de Posgrado e Investigación, ESIA-Unidad Ticomán. Av. Ticomán No. 600 Col. San José Ticomán. Del. Gustavo A. Madero, C.P. 07340 México, D.F.

collaborators (1982). Ferric iron of the ferromagnesians was calculated using the charge balance equation described by Papike *et al.* (1974).

Whole-rock analyses and trace elements, including the REE elements, were carried by X-ray Fluorescence Spectrometry and by Inductively Coupled Plasma-Atomic Emission Spectrometry at the Centre des Recherches Pétrographiques et Géochimiques (C.R.P.G.) of Nancy, France, with SIEMENS SR1, SIEMENS SRS 200 and Jovin-Yvon AJY48P 20 spectrometers, with analytical errors of 0.5 ppm for contents < 10 ppm and 5% for contents > 10 ppm, after the analytical method of Govindaraju and Mevell (1987).

Nd/Sm and Rb/Sr isotopic data were analysed by isotopic dilution at the Saint Etienne University's Geology Laboratory using a CAMECA TSN 206 mass spectrometer. Standards values are:

Standard E&A : 0.70799 ± 0.00004 normalized to $^{86}Sr/^{88}Sr = 0.1194$

Standard BCR 1: 0.512638 ± 0.00003 normalized to $^{146}Nd/^{144}Nd = 0.7219$

Initial ratios were calculated with the decay constants:

λ Rb = 1.42 x 10^{-11} years^{-1} for the ^{87}Rb

λ Sm = 6.54 x 10^{-12} years^{-1} for the ^{147}Sm

The Epsilon Sr was calculated with respect to an uniform reservoir of $^{87}Sr/^{86}Sr = 0.7045$ and $^{87}Rb/^{86}Sr = 0.0827$. The Epsilon Nd was calculated respect to a chondritic uniform reservoir of $^{143}Nd/^{144}Nd = 0.512638$ and $^{147}Sm/^{144}Nd = 0.1967$ (De Paolo, 1988).

K/Ar radiometric age of amphibole from one ankaramitic sample was carried out in a THN205E mass spectrometer at (C.R.P.G.) of Nancy, France. K was determined by atomic absorption and Ar by isotopic dilution using ^{38}Ar as spike. Decay constants used were (Zimmermann *et al.*, 1985):

$\lambda\beta$ =4.962 x 10^{-10} years^{-1}

$\lambda\gamma$ =0.581 x 10^{-10} years^{-1}

^{40}Ar=0.01167 % K

GEOLOGICAL SETTING

The Sierra de Guanajuato is a segment of the tectonostratigraphic Guerrero terrane, exposed in central Mexico (Figure 1), which consist of accreted Late Jurassic-Early Cretaceous island arc volcano-sedimentary sequences (Campa and Coney, 1983; Campa, 1985).

Monod *et al.* (1990), Lapierre *et al.* (1992), and Ortiz *et al.* (1992) have proposed that the Mesozoic stratigraphy of the Sierra de Guanajuato is formed by a Late Jurassic-Early Cretaceous comagmatic volcano-plutonic sequence named the Guanajuato Magmatic Sequence. It is formed by tholeiitic ultramafic-mafic cumulate rocks, diorites, tonalites, a dike complex and basaltic pillow-lavas, belonging to an intra-oceanic island arc. The arc was thrusted over the Arperos Formation, a contemporaneous volcano-sedimentary sequence formed by greywackes, quartzites, micritic limestones,

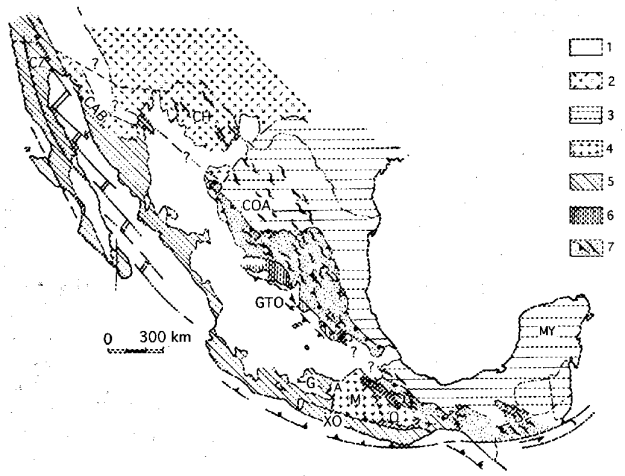

Figure 1. Tectonostratigraphic terranes of Mexico (after Campa, 1985), and location of the Guanajuato segment (GTO).
1. Cenozoic volcanic rocks; 2. Southwestern end of the North American Craton; 3. Eastern Appalachian basements and Gulf of Mexico Mesozoic transgressive overlap sequence; 4. Continental allochtonous blocks immersed in western collage; 5. Western Cordillera collage of island arc and other fragments of igneous oceanic crust and melange; 6. Late Jurassic-Early Cretaceous turbidite belt; 7. Mexican Thrust Belt.
Terranes: G: Guerrero; J: Juárez; M: Mixteca; O: Oaxaca; CH: Chihuahua; MY: Maya; XO: Xolapa; CAB: Caborca; COA: Coahuila.

radiolarian cherts, black shales and conglomerates with basalts, diabases and rare volcaniclastic rocks at the base.

This volcano-sedimentary sequence is a remnant of intra-plate seamounts and basinal facies of an oceanic basin that has suffered a hot-spot magmatism during Early Cretaceous age (Ortiz-Hernández, submitted). Metamorphic parageneses of the Guanajuato magmatic sequence and the Arperos Formation are typical of low-grade metamorphic terranes, ranging from greenschist to prehnite-pumpellyite facies. Morever, magmatic textures are generally preserved, except at tectonic contacts.

For the geological descriptions, petrographic and geochemical characteristics of the two sequences forming the framework of the Sierra de Guanajuato, see Monod *et al.* (1990), Lapierre *et al.* (1992), and Ortiz *et al.* (1992).

Ankaramites occur at the base of the Guanajuato Magmatic Sequence, intruding the ultramafic cumulate rocks (Figure 2), at the San Juan de Otates stream. The geological cross-section accross the El Maguey tungsten mine and the San Juan de Otates stream show tectonic sheets of serpentinized wherlites, olivine-clinopyroxenites and cumulate gabros that are crosscut by a great variety of lithologies including mafic, acidic and rodingitic dikes, by small bodies of dioritic to monzonitic rocks, and also by intrusive magmatic breccias. This sequence is thrusted to the NE over the Arperos Formation (Figure 3) that shows the imprint of a polyphase penetrative deformation.

Ankaramites are present as massive, scarce, undeformed dark dikes (± 1 m in tickness), without chilled margins,

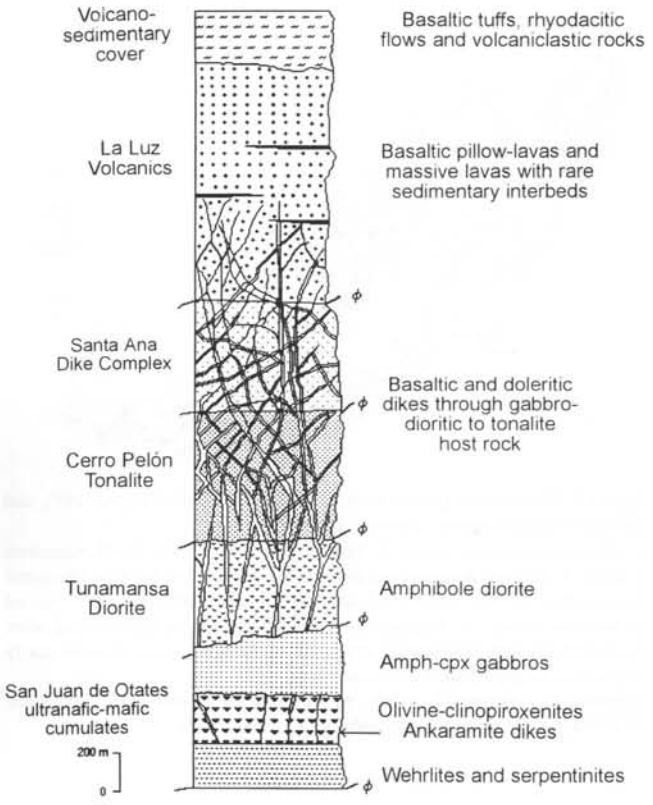

Figure 2. Guanajuato magmatic sequence reconstructed lithostratigraphy showing the ankaramite dikes occurrence.
ϕ = Tectonic contact

emplaced into fractures with orientation N 170° E; 60° W in the ultramafic rocks (Figure 4).

A potassium-argon date on amphibole from one ankaramite sample yield a Pliensbachian age of 195 Ma (Table 1), that is not representative of their crystallization age, because it cuts Early Cretaceous rocks. Whole-rock K-Ar radiometric ages of mafic and ultramafic cumulate rocks of the Guanajuato magmatic sequence were reported by Lapierre *et al.* (1992) and yield 112.8 ± 6.8 Ma for a gabbro and 113 ± 7 Ma for a clinopyroxenite.

On the other hand, K-Ar dates of K-bearing minerals in regionally metamorphosed rocks form a metamorphic veil that obscures the time of original crystallization of such rocks (Faure, 1977). An Early Cretaceous age of ankaramites is considered as probably.

PETROGRAPHIC CHARACTERISTICS AND CHEMICAL COMPOSITION OF MINERALS

The Guanajuato ankaramites are melanocratic rocks with abundant clinopyroxene (±40 modal %), and subordinated olivine crystals (8 modal %). In thin section (Figure 5), these

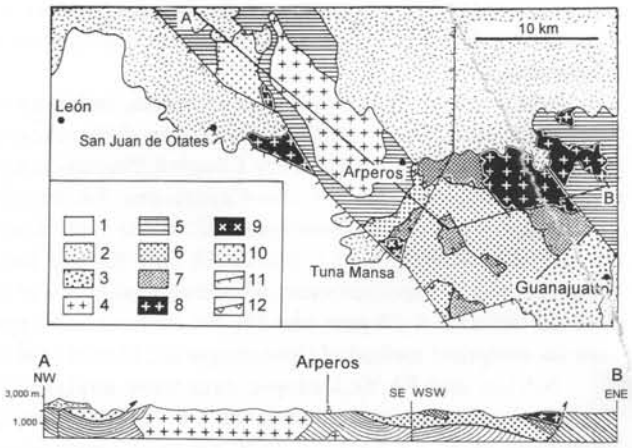

Figure 3. Simplified geological map of the Sierra de Guanajuato (central Mexico) between San Juan de Otates town and Guanajuato city.
1. Quaternary sediments; 2. Tertiary and Plio-Quaternary volcanic rocks; 3. Guanajuato red conglomerate; 4. Tertiary granite; 5. Arperos Formation; 6. La Luz volcanic unit; 7. Santa Ana dike complex; 8. Cerro Pelón tonalite; 9. Tunamansa diorite; 10. San Juan de Otates ultramafic-mafic cumulate rocks; 11. Normal fault; 12. Thrust.

rocks display subhedral, zoned clinopyroxene phenocrysts ranging in composition from diopside ($Wo_{45.6-48.0}$ $En_{42.8-48.9}$ $Fs_{4.9-9.7}$) in the core, through salite ($Wo_{43.9-47.8}$ $En_{40.3-45.2}$ $Fs_{10.1-13.4}$) in the rim. Endiopside ($Wo_{44.2}$ $En_{46.7}$ $Fs_{9.1}$) and augite ($Wo_{44.4}$ $En_{44.2}$ $Fs_{11.2}$) are rare (Table 2). Analyses of clinopyroxene population (n = 45) show that 45% are salites, 42% diopsides, 9% augites and only 4% are endiopsides. The range of #Mg=(100Mg(Mg/Fe*)) of the clinopyroxenes decreases from diopsides (91-82) and endiopsides (84) to salite (82-76) and augite (80), suggesting a process of mineral fractionation. The clinopyroxene rims display a slightly iron enrichment, represented by a salitic trend (Figure 6). Anhedral olivine crystal are replaced by aggregates of pumpellyite, smectites or chlorite. The oxides, present as inclusions in the olivine, are magnesiochromites ($Mg > Fe^{2+}$; $Cr > Al$)

Figure 4. Ankaramitic dike intruding ultramafic cumulate rocks at the San Juan de Otates stream. Handle as scale.

Table 1. K/Ar isotopic data from one ankaramite dike.

SAMPLE	ANALYSED MATERIAL	K (%)	^{40}Ar rad. (10^{-6}cm^3/g)	^{40}Ar atm. (%)	AGE (±2σ Ma)
MA-7	Amphibole	0.40	3.193	66.60	194.7±7.5

with #Cr= (Cr/(Cr+Al) = 0.80) (Table 3), that suggest a highly refractory source, different to MORB sources, that have #Cr = <0.65 (Dick and Bullen, 1986). These spinels are similar to spinels type III of Dick and Bullen (1986), restricted to boninites, stratiform complex, zoned Alaskan complex and oceanic plateau basalts. Small quantities (5 modal %) of low-silica ($6.27 \leq Si \leq 6.29$), aluminous, calcic amphibole phenocrysts ($(Ca+Na)_B \geq 1.34$; $Na_B < 0.67$) occur. These range in composition from pargasite in the cores to pargasitic hornblende in the rims ($0.72 < Mg/(Mg+Fe^{2+}< 0.73$), or from magnesio-hastingsite to magnesio-hastingsitic hornblende (6.10 wt% < Si < 6.30 wt% and $0.80 < Mg/(Mg+Fe^{2+}) < 0.81$); (Leake, 1978; Table 3 and Figure 7). The groundmass of the rocks is formed by subhedral to euhedral microphenocrysts of calcic-amphibole ranging in composition from pargasitic hornblende to pargasite (Leake, 1978; Table 3), rare albite (Ab_{97}), and minor interstitial prehnite and chlorite. Both, the amphibole phenocrysts and the microphenocrysts show a ferromagnesian normal trend in the Ca-Mg-Fe diagram (Figure 6), characterized by an increase of Mg-Fe as a function of Ca contents. Petrographic characteristics preclude a cumulate origin for these rocks.

Crystallization order of the ankaramite dikes is chromian spinel—>olivine—>clinopyroxene—>amphibole—>plagioclase. The primitive nature of the rocks is reflected by the magnesiochromite inclusions in the olivine and by the high #Mg of the clinopyroxenes. Amphiboles were formed probably by replacement of clinopyroxene during an early stage of hydration of the ankaramitic magma. Albitic composition of the plagioclase resulted from the low-grade metamorphic event (prehnite-pumpellyite facies) affecting the dikes.

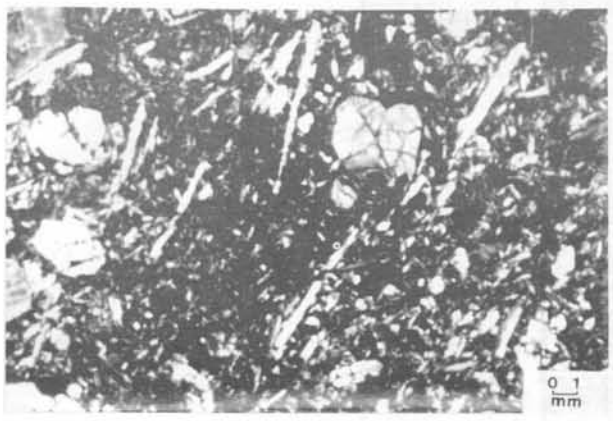

Figure 5. Photomicrograph of ankaramite rock showing zoned clinopyroxene and amphibole phenocrysts in a groundmass of albite, amphibole and magnesiochromites.

Clinopyroxenes of Guanajuato ankaramites have relatively high TiO_2 and Al_2O_3 contents. They are rich in SiO_2, MgO, and CaO, but they are Na_2O-poor (Table 2), which is a typical feature of orogenic magma series (Marcelot *et al.*, 1988). Diopsides are more Cr_2O_3-rich than the other clinopyroxenes. They show a decrease in Cr_2O_3 as a function of Al_2O_3 and TiO_2 (Figure 8), that suggests the role of the salitic trend and mineral fractionation. Other non-quadrilateral components (Papike *et al.*, 1974) for these clinopyroxenes are the Ca-Tschermak molecule ($CaAl_2SiO_6$), indicating an important role of coupled Al^{VI}-Al^{IV} substitutions (Figure 9). This type of substitution is typical of orogenic series and is favored by the lowering of silica activity in the melt (Marcelot *et al.*, 1988). Al^{IV}/Al^{VI} ratios range from 0.70-4.62 for the diopsides, 0.87-2.13 for the salites, 1.17-1.54 for the augites, and 0.82-1.92 for the endiopsides, indicating that they are not mantle relicts. Al/Ti ratio of these ferromagnesians range from 2.5 to 37.75.

Amphiboles in the ankaramites are appreciably more aluminous ($1.69 < Al^{IV} < 1.89$) than those hornblendes of island arc volcanic rocks (Al^{IV}> 1.5-1.6). A NaM_4-A-Al^{IV} ternary plot shows that other components for these amphiboles are the pargasite-hastingsite molecule ($NaCa_2Mg_4AlSi_6Al_2$-$NaCa_2Mg_4Fe^{3+}Si_6Al_2$) (Figure 10). The change from pargasitic to hastingsitic composition is represented by an increase of NaM_4 and Fe^{3+}, and by a decrease of Ti and Al^{IV} in the structural formulae. This transition is interpreted in terms of variations of fO_2 in the magma during the evolution of a hydrous melt.

WHOLE-ROCK GEOCHEMISTRY

Only two whole-rock analyses of ankaramitic rocks of Guanajuato were carried out. They are low-silica, high MgO (8 wt% < MgO < 10 wt% at 47-49 wt% of SiO_2), Cr, Ni and V rocks (Table 4), with high Cr/Ni (5-6), and Sc/Ni (0.73-0.92) ratios, characteristic of ankaramitic arc suites (Bardsell and Berry, 1990). They are relatively poor in Al_2O_3, but rich in CaO, Na_2O, Sr, K, Rb and Ba (Table 4). These relatively high values for alkaline elements are linked to rock alteration

Table 2. Microprobe analyses of clinopyroxene phenocrysts (wt%) from Guanajuato ankaramites (Sample MA-7). Structural formulae calculated by stoichiometry to 6 oxygens and 4 cations.

	1	2	3	4	5	6	7	8	9	10	11	12	13	14	15	16	17	18	19	20	21	22	23
SiO_2	53.66	53.25	53.62	52.96	53.92	51.09	54.12	53.26	53.28	50.26	51.88	51.3	51.38	50.75	50.1	52.43	52.33	53.03	51.29	50.5	51.12	51.98	51.2
TiO_2	0.13	0.14	0.12	0.19	0.07	0.35	0.07	0.13	0.22	0.47	0.21	0.35	0.51	0.8	0.66	0.24	0.14	0.18	0.39	0.54	0.49	0.37	0.56
Al_2O_3	1.05	1.93	1.09	1.85	1.04	3.43	1.17	3.08	1.79	4.35	3.85	3.98	4.54	5.21	5.13	2.97	2.07	2.09	3.88	3.9	3.9	2.53	3.68
FeO	3.6	3.54	3.01	3.93	3.1	6.54	3.15	3.03	4.83	6.2	5.61	6.44	6.56	7.01	7.15	4.67	3.97	3.43	6.63	6.84	6.59	6.49	6.65
Cr_2O_3	0.68	0.74	0.9	0.57	0.64	0.15	0.69	0.65	0.17	0.01	0.19	0	0.02	0	0.01	0.26	0.63	0.62	0.12	0.09	0	0	0
MnO	0.17	0.08	0.05	0.01	0	0.22	0.06	0.08	0.17	0.22	0.06	0.15	0.14	0.12	0.09	0.1	0.05	0.14	0.14	0.17	0.05	0.07	0.07
NiO	0.06	0.07	0.03	0	0.06	0.04	0.05	0.13	0	0.09	0	0	0	0.07	0	0.04	0	0	0	0	0.06	0	0.02
MgO	17.07	16.62	17.15	16.47	17.33	14.45	17.05	16.93	15.87	15.3	15	14.9	13.88	13.56	13.75	16.13	16.33	16.45	14.3	14.09	14.83	14.98	14.22
CaO	23.33	23.14	22.83	22.89	22.81	22.5	22.72	22.58	22.6	22.2	22.17	21.96	22.43	21.86	21.9	22.32	23.35	23.45	22.9	22.9	21.73	21.83	22.64
Na_2O	0.18	0.21	0.23	0.2	0.19	0.24	0.17	0.12	0.18	0.26	0.22	0.27	0.25	0.28	0.31	0.25	0.19	0.2	0.32	0.3	0.29	0.93	0.35
TOTAL	99.93	99.72	99.03	99.07	99.16	99.01	99.25	99.99	99.11	99.36	99.19	99.35	99.71	99.66	99.1	99.41	99.06	99.59	99.97	99.33	99.06	99.18	99.39
Si	1.963	1.95	1.971	1.953	1.967	1.913	1.97	1.935	1.968	1.87	1.919	1.904	1.901	1.881	1.872	1.93	1.936	1.945	1.9	1.888	1.903	1.936	1.906
Ti	0.004	0.004	0.003	0.005	0.018	0.004	0.019	0.004	0.005	0.013	0.006	0.01	0.014	0.022	0.019	0.007	0.004	0.005	0.011	0.015	0.014	0.01	0.016
Al	0.045	0.083	0.047	0.08	0.045	0.151	0.05	0.132	0.078	0.191	0.168	0.174	0.198	0.228	0.226	0.129	0.09	0.09	0.169	0.172	0.171	0.111	0.161
Fe	0.11	0.108	0.093	0.121	0.095	0.205	0.096	0.092	0.149	0.193	0.174	0.2	0.203	0.217	0.223	0.144	0.123	0.105	0.205	0.214	0.205	0.202	0.207
Cr	0.02	0.021	0.026	0.017	0.018	0.004	0.02	0.019	0.005	0	0.006	0	0.001	0	0	0.008	0.018	0.018	0.004	0.003	0	0	0
Mn	0.005	0.002	0.002	0	0	0.007	0.002	0.002	0.005	0.007	0.002	0.005	0.004	0.004	0.003	0.003	0.002	0.004	0.004	0.005	0.002	0.002	0.002
Ni	0.002	0.002	0.001	0	0.002	0.001	0.001	0.004	0	0.003	0	0	0	0.002	0	0.001	0	0	0	0	0.002	0	0.001
Mg	0.931	0.907	0.94	0.905	0.942	0.807	0.925	0.917	0.874	0.849	0.827	0.824	0.766	0.749	0.766	0.885	0.901	0.899	0.79	0.785	0.823	0.832	0.789
Ca	0.915	0.908	0.899	0.904	0.891	0.903	0.886	0.879	0.895	0.885	0.879	0.873	0.889	0.868	0.877	0.88	0.926	0.922	0.909	0.917	0.867	0.871	0.903
Na	0.013	0.015	0.016	0.014	0.013	0.017	0.012	0.008	0.013	0.019	0.016	0.019	0.018	0.02	0.022	0.018	0.014	0.014	0.023	0.022	0.021	0.067	0.025
TOTAL	4.008	4	3.998	3.999	3.991	4.012	3.981	3.992	3.992	4.03	3.997	4.009	3.994	3.991	4.008	4.005	4.014	4.002	4.015	4.021	4.008	4.031	4.01
%En	47.5	47.1	48.6	46.9	48.9	42	48.5	48.5	45.4	43.9	44	43.3	41.1	40.8	41	46.3	46.2	46.6	41.4	40.9	43.4	43.6	41.5
%Fs	5.9	5.8	4.9	6.3	4.9	11	5.1	5	8	10.3	9.3	10.8	11.1	12	12.1	7.7	6.4	5.7	11	11.4	10.9	10.7	11
%Wo	46.6	47.1	46.5	46.8	46.2	47	46.4	46.5	46.6	45.8	46.7	45.9	47.8	47.2	46.9	46	47.4	47.7	47.6	47.7	45.7	45.7	47.5
Al^{IV}	0.037	0.05	0.029	0.047	0.033	0.087	0.03	0.065	0.032	0.13	0.081	0.096	0.099	0.119	0.128	0.07	0.064	0.055	0.1	0.112	0.097	0.064	0.094
Al^{VI}	0.008	0.033	0.018	0.033	0.012	0.064	0.02	0.067	0.046	0.061	0.087	0.078	0.099	0.109	0.098	0.059	0.026	0.035	0.069	0.06	0.074	0.047	0.067
#Mg	87	89	87	88	91	80	91	91	85	81	83	80	79	78	77	86	88	86	79	79	80	80	85

	24	25	26	27	28	29	30	31	32	33	34	35	36	37	38	39	40	41	42	43	44	45
SiO_2	51.89	51.2	50.88	52.24	51.89	51.36	50.07	50.18	52.9	51.5	51.92	52.21	53.1	52.69	51.83	53.04	53.25	52.11	50.68	52.06	50.08	51.91
TiO_2	0.35	0.41	0.32	0.26	0.32	0.45	0.65	0.81	0.18	0.44	0.31	0.3	0.41	0.34	0.4	0.29	0.23	0.34	0.61	0.26	0.69	0.33
Al_2O_3	2.61	3.22	3.19	2	2.89	3.27	4.19	5.13	1.69	3.68	3.22	2.28	3.25	2.87	3.17	1.93	2.36	2.54	4.65	2.33	4.37	2.55
FeO	5.3	6.07	5.19	5.77	5.29	5.62	7.08	7.79	5.63	6.03	6.84	6.53	6.69	6.44	6.11	6.37	6.09	6.26	6.83	7.69	7.42	5.85
Cr_2O_3	0.27	0	0.29	0.26	0.2	0.03	0	0	0.1	0.09	0	0.09	0	0.12	0.16	0.1	0	0	0	0	0.07	0
MnO	0.17	0.08	0.14	0.19	0.17	0.11	0.13	0.19	0.15	0.13	0.18	0.29	0.26	0.25	0.11	0.17	0.16	0.14	0.15	0.12	0.26	0.01
NiO	0	0	0.01	0	0	0.19	0.05	0.04	0	0.11	0	0	0	0	0	0	0	0	0	0	0.01	0
MgO	15.19	15.73	15.77	15.78	15.23	14.9	14.06	13.45	16.67	14.6	15.32	15.82	15.2	15.5	15.53	16.26	16.07	15.61	13.92	15.18	14.48	15.54
CaO	22.94	22.69	23.43	22.31	23.31	23.19	22.47	21.45	21.98	22.56	21.46	21.37	21.87	22.4	21.88	21.81	21.54	22,32	22.33	20.98	21.48	23.01
Na_2O	0.31	0.24	0.26	0.2	0.21	0.27	0.31	0.33	0.21	0.25	0.18	0.17	0.22	0.18	0.27	0.19	0.26	0.17	0.29	0.4	0.33	0.19
TOTAL	99.03	99.64	99.48	99.01	99.51	99.39	99.01	99.37	99.51	99.39	99.43	99.06	100.01	100.79	99.46	100.16	99.96	99.49	99.46	99.02	99.19	99.39

Si	1.93	1.898	1.89	1.943	1.921	1.908	1.878	1.873	1.952	1.906	1.924	1.941	1.935	1.928	1.918	1.949	1.954	1.931	1.885	1.944	1.874	1.926
Ti	0.01	0.011	0.009	0.007	0.009	0.013	0.018	0.023	0.005	0.012	0.009	0.008	0.011	0.009	0.011	0.008	0.006	0.009	0.017	0.007	0.019	0.009
Al	0.114	0.141	0.14	0.088	0.126	0.143	0.185	0.226	0.073	0.162	0.141	0.1	0.14	0.124	0.138	0.084	0.102	0.111	0.204	0.103	0.193	0.112
Fe	0.165	0.188	0.161	0.179	0.164	0.175	0.222	0.243	0.174	0.188	0.212	0.203	0.204	0.197	0.189	0.196	0.187	0.194	0.212	0.24	0.232	0.182
Cr	0.008	0	0.009	0.008	0.006	0.001	0	0	0.003	0.003	0	0.003	0	0.003	0.005	0.003	0	0	0	0	0.002	0
Mn	0.005	0.003	0.004	0.006	0.005	0.003	0.004	0.006	0.005	0.004	0.006	0.009	0.008	0.008	0.003	0.005	0.005	0.004	0.005	0.004	0.008	0
Ni	0	0	0	0	0	0.006	0.002	0.001	0	0.003	0	0	0	0	0	0	0	0	0	0	0	0
Mg	0.842	0.869	0.873	0.875	0.841	0.825	0.786	0.749	0.917	0.812	0.846	0.877	0.826	0.845	0.857	0.891	0.879	0.862	0.772	0.845	0.808	0.859
Ca	0.914	0.901	0.932	0.889	0.925	0.923	0.903	0.858	0.869	0.901	0.852	0.851	0.854	0.878	0.868	0.859	0.847	0.886	0.89	0.84	0.861	0.915
Na	0.022	0.017	0.019	0.014	0.015	0.019	0.023	0.024	0.015	0.018	0.013	0.012	0.016	0.013	0.019	0.014	0.018	0.012	0.021	0.029	0.024	0.014
TOTAL	4.01	4.028	4.037	4.009	4.012	4.016	4.021	4.003	4.013	4.009	4.003	4.004	3.994	4.005	4.008	4.009	3.998	4.009	4.006	4.012	4.021	4.017

%En	43.7	44.3	44.3	44.9	43.5	42.8	41	40.3	46.7	42.6	44.2	45.2	43.7	43.8	44.7	45.7	45.8	44.3	41.1	43.8	42.3	43.9
%Fs	8.8	9.7	8.4	9.5	8.7	9.2	11.8	13.4	9.1	10.1	11.4	10.9	11.2	10.6	10	10.3	10	10.2	11.6	12.7	12.6	9.3
%Wo	47.5	46	47.3	45.6	47.8	48	47.2	46.3	44.2	47.3	44.4	43.9	45.1	45.6	45.3	44	44.2	45.5	47.3	43.5	45.1	46.8
Al^{IV}	0.07	0.102	0.11	0.057	0.079	0.092	0.122	0.127	0.048	0.094	0.076	0.059	0.065	0.072	0.082	0.051	0.046	0.069	0.115	0.056	0.126	0.074
Al^{VI}	0.044	0.039	0.03	0.031	0.047	0.051	0.063	0.099	0.025	0.068	0.065	0.041	0.075	0.052	0.056	0.033	0.056	0.042	0.089	0.047	0.067	0.038
#Mg	84	82	84	83	84	83	78	76	84	81	80	81	80	81	82	82	82	82	78	78	78	83

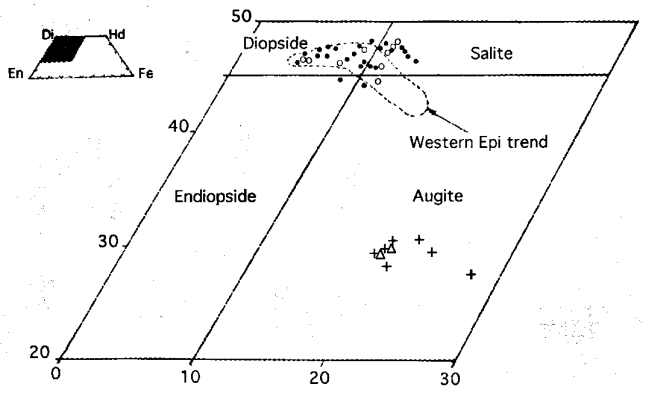

Figure 6. Di-Hd-En-Fs diagram showing the clinopyroxene and amphibole composition from the Guanajuato ankaramites. Field from the Western Epi ankaramites, after Bardsell and Berry (1990).
Full circle: clinopyroxene core
circle: clinopyroxene rim
cross: amphibole phenocryst
triangle: amphibole microphenocryst.

(especially the case of DM-11 sample). Mg number (100Mg/(Mg+Fe*)) for the ankaramites range from 52 to 55, decreasing inversely with the silica content. Zr/Y ratios (>3) and Ti/V ratios (< 20) are in the range reported for volcanic rocks from modern and ancient island arcs. Their REE chondritic-normalized patterns (Evensen *et al.*, 1978) are slightly enriched in LREE (Figure 11A), with $(La/Yb)_N$ ratios not exceeding 3 (Table 4) and have a small negative Eu anomaly ($0.88 < Eu/Eu^* < 0.93$). Western Epi ankaramites have similar $2.8 < (La/Yb)_N < 3.3$ ratios, with relatively unfractionated patterns (Bardsell and Berry, 1990). This relatively unfractionated REE abundance pattern of the Guanajuato ankaramites ($10x < REE < 40x$) suggests that these rocks are primitive melts.

Table 3. Microprobe analyses of amphibole phenocrysts and microphenocrysts (1 to 9), plagioclase microlite (10), and Cr-spinel inclusions in olivine (11 and 12) from the Guanajuato ankaramites (sample MA-7). Structural formulae of amphiboles calculated using the method of Robinson *et al.* (1982). Fe partition calculated using the charge balance equation of Papike *et al.* (1974). Structural formulae of plagioclase and spinel calculated by stoichiometry to 8 oxygens and 4 cations, and 32 oxygens and 24 cations, respectively.

	1	2	3	4	5	6	7	8	9	10	11	12
SiO_2	41.4	42.73	42.12	42.17	41.59	43.23	42.24	41.46	41.87	68.53		
TiO_2	1.89	1.77	1.48	1.43	1.94	0.47	1.73	1.73	1.94		0.57	0.53
Al_2O_3	13.3	12.44	12.69	13.25	13.27	13.32	12.43	13.37	12.38	20.31	7.73	7.82
Cr_2O_3											46.84	47.02
FeO	10.88	11.06	10.94	10.5	9.85	11.6	10.74	13.01	12.05	0.27	30.47	29.79
MnO	0.12	0.13	0.1	0.1	0.1	0.21	0.04	0.44	0.23		0.55	0.18
MgO	14.04	14.35	13.92	13.15	14.23	13.34	14.76	12.33	13.79		10.31	10.53
CaO	11.64	11.52	11.55	11.73	11.75	11.62	11.75	10.54	10.48	0.27		
Na_2O	2.27	2.42	2.32	2.19	2.4	2	2.33	2.5	2.56	10.77		
K_2O	0.47	0.46	0.63	0.61	0.58	0.4	0.48	0.24	0.31	0.28		
TOTAL	96.01	96.88	95.75	95.13	95.71	96.19	96.7	95.6	95.61	100.43	96.47	95.87
Si	6.14	6.293	6.277	6.277	6.128	6.309	6.241	6.108	6.281	2.978		
Ti	0.211	0.196	0.166	0.16	0.215	0.052	0.191	0.192	0.219		0.117	0.109
Al										1.04	2.488	2.527
Al^{IV}	1.86	1.707	1.723	1.723	1.872	1.691	1.759	1.892	1.719			
Al^{VI}	0.466	0.453	0.507	0.602	0.433	0.601	0.396	0.431	0.471			
Cr											10.11	10.188
Fe										0.01		
Fe^{2+}	0.989	1.113	1.127	0.997	0.711	0.708	0.951	0.625	1.221		3.792	3.764
Fe^{3+}	0.226	0.084	0.094	0.31	0.503	0.708	0.226	0.978	0.006		3.169	3.066
Mn	0.015	0.016	0.013	0.013	0.012	0.026	0.005	0.055	0.029		0.127	0.042
Mg	3.104	3.15	3.092	2.918	3.125	2.902	3.235	2.708	3.084		4.197	4.303
Ca	1.85	1.818	1.845	1.871	1.855	1.817	1.852	1.664	1.685	0.013		
Na	0.653	0.691	0.67	0.632	0.686	0.566	0.664	0.714	0.745	0.907		
K	0.089	0.086	0.12	0.116	0.109	0.074	0.09	0.045	0.059	0.016		
Na_B	0	0	0	0.129	0.145	0.183	0	0.336	0			
TOTAL										4.964	24	23.999
%An										1.3		
%Ab										97		
%Or										1.7		
%Magn											20.1	19.4
%Herc											15.8	16
%Chrom											64.1	64.6
#Cr											0.8	0.8
$Mg/(Mg + Fe^{2+})$											0.52	0.53

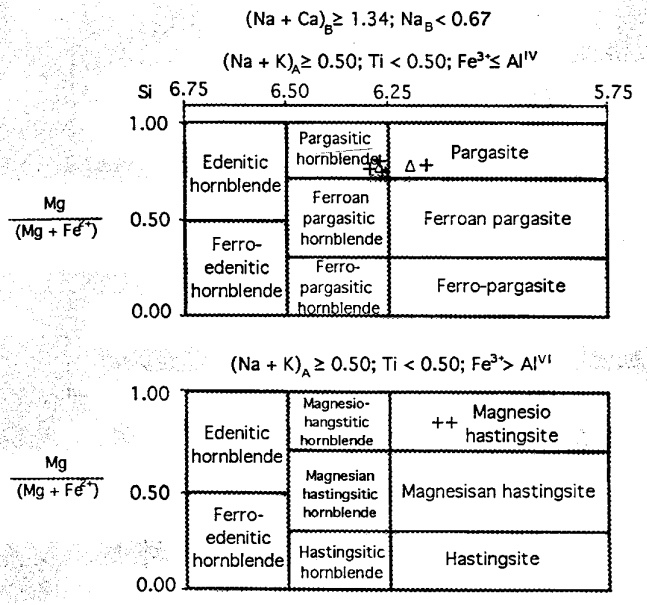

Figure 7. Si-Mg/(Mg + Fe^{2+}) diagram (after Leake, 1978) showing the ankaramite amphibole composition.

MORB-normalized spidergrams (Pearce, 1983) show an enrichment in large-ion lithophile elements (LILE= Sr, K, Rb, Ba), and a depletion in high-field strength elements (HFSE = Ti, Zr, Y) (Figure 11B). This pattern is characteristic of subalkaline magmas formed in convergent margins settings (Pearce, 1983).

Preliminary Nd/Sm and Rb/Sr isotopic studies on one ankaramitic dike show an initial $^{143}Nd/^{144}Nd$ ratio of 0.513009±16 (Table 5) that corresponds to an Epsilon Nd (T=110 Ma)=+7.22, which precludes significant crustal contamination and is consistent with a HFSE-depleted arc-magma source, where fluids derived from a subducting slab induce further melting in an overlying peridotitic source. This

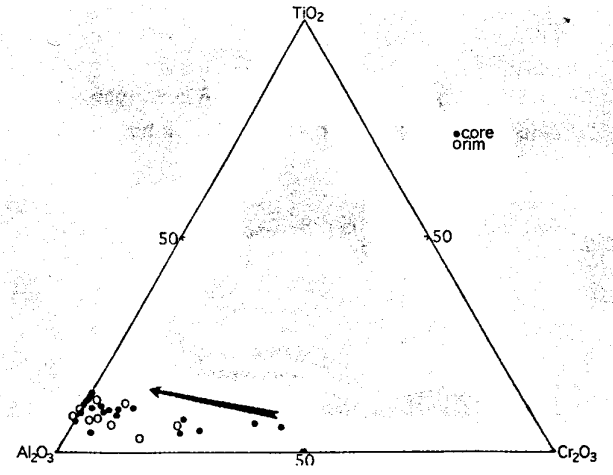

Figure 8. TiO_2-Al_2O_3-Cr_2O_3 ternary plot showing the evolution of the ankaramite clinopyroxenes. Arrow shows the fractional trend of these ferromagnesians.

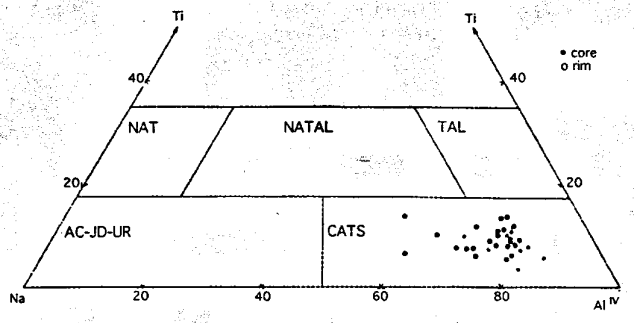

Figure 9. Ti-NaM_4-Al^{IV} ternary plot (after Papike *et al.*, 1974) showing the ankaramite clinopyroxene classification.
NAT = $NaT_{i0.5}R^{2+}{}_{0.5}Si_2O_6$; NATAL = $NaTiSiAlO_6$; TAL = $CaTiAl_2O_6$; CATS = $CaAl_2SiO_6$, and $CAFeAlSiO_6$; AC = $NaFeSi_2O_6$; JD = $NaAlSiO_6$; UR = $NaCrSi_2O_6$.

value is in the range of values reported for the Upper Jurassic-Early Cretaceous tholeiitic magmatic sequence (+7 < ε_{Nd} (T=122 Ma) < +9; Lapierre *et al.*, 1992), and for the Aptian-Albian calc-alkaline monzonitic rocks (ε_{Nd}(T= 100 Ma)= +6.44) (Stein *et al.*, 1994), intruding the above mentioned sequence. On the other hand, the $^{87}Sr/^{86}Sr$ ratio is 0.703545 ± 30 that correspond to an Epsilon Sr (T=110 Ma)= -11.78 (Table 5), which is consistent with a slight enrichment in radiogenic Sr of the rock.

DISCUSSION AND CONCLUSIONS

At the Guanajuato segment two contrasting arc magma series of Early Cretaceous age exist: the pristine tholeiitic magmatic sequence of Guanajuato and the calc-alkaline and mature tholeiitic magmatic breccias (Ortiz-Hernández, submitted). The calc-alkaline series is represented by small dioritic to monzodioritic bodies and magmatic breccias intruding the ultramafic cumulate rocks considered as the lower member of this sequence, and the tholeiitic mature series occurs mainly as

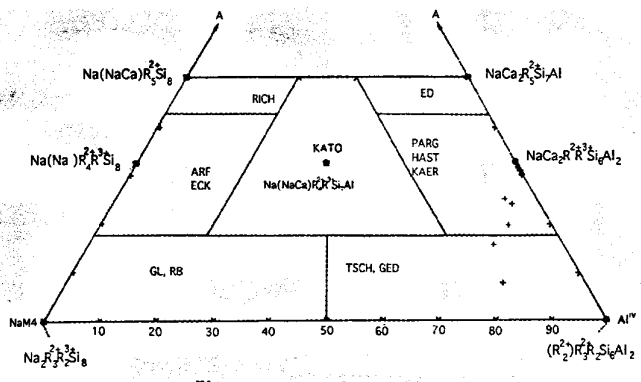

Figure 10. NaM_4-A-Al^{IV} ternary plot (after Papike *et al.*, 1974) showing the classification of ankaramite amphibole end-members. RICH = Richterite; ED = Edenite; ARF-ECK = Arfvendsonite-Eckermanite; KATO = Katophorite; PARG-HAST-KAER = Pargasite-Hastingsite-Kaersutite; GL-RB = Glaucophane-Riebeckite; TSCH-GED = Tschermakite-Gedrite.
cross = amphibole phenocryst
triangle = amphibole microphenocryst.

Table 4. Chemical analyses for the ankaramite dikes of Guanajuato. Major elements in wt% and trace elements in ppm.

	MA-7	DM-11
SiO_2	47.14	49.59
TiO_2	0.79	0.8
Al_2O_3	13.01	13.78
Fe_2O_3	10.73	10.89
MnO	0.17	0.17
MgO	9.55	8.35
CaO	10.58	8.71
Na_2O	3.27	4
K_2O	0.12	0.76
P_2O5	0.35	0.25
P.I.	3.24	2.64
TOTAL	98.95	99.94
Mg number	55	52
Rb	8	14
Sr	540	855
Ba	134	545
Cr	309	274
Ni	51	52
V	247	252
Sc	47	38
Zr	63	73
Y	21	20
La	7.88	7.96
Ce	25.48	22.79
Nd	13.59	14.17
Sm	3.67	4.02
Eu	1.06	1.21
Gd	3.57	3.88
Dy	3.27	3.46
Er	2.02	1.75
Yb	1.75	1.95
Lu	0.21	0.34
(La/Yb)N	3	2.75

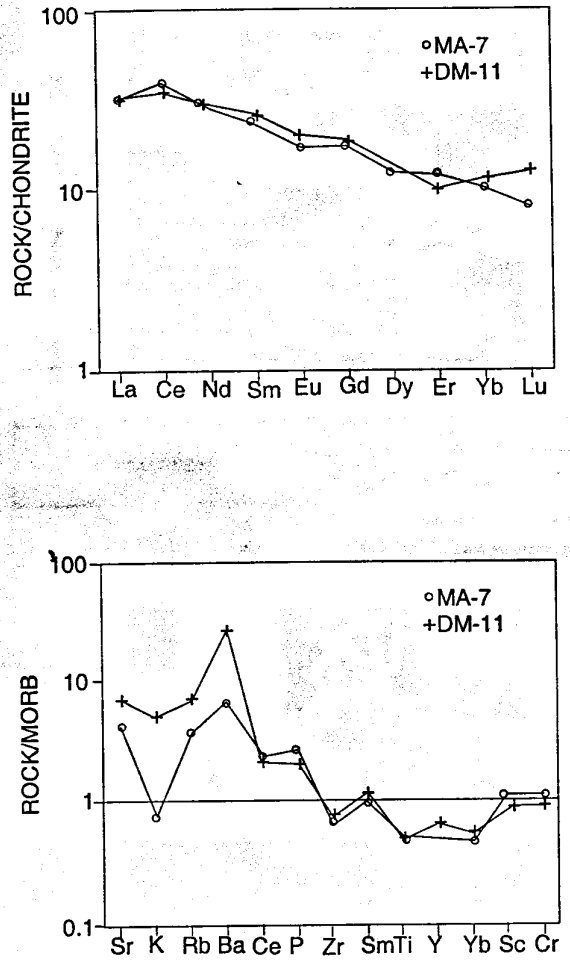

Figure 11. A. Rare earth patterns normalized to chondrites (Evensen *et al.*, 1978) for the Guanajuato ankaramites. B. Diagramas normalized to MORB (Pearce, 1983) for the Guanajuato ankaramites.

disrupted dikes into the dike complex, at the top of the magmatic succession.

On the other hand, field evidence shows that the ankaramitic magmatism is:

- Late in the arc evolution because they intrude the basal ultramafic cumulate pile of the tholeiitic Guanajuato Magmatic Sequence.

- Probably coeval with Aptian-Albian mature tholeiitic and calc-alkaline dioritic to monzodioritic magmatic breccias

Table 5.- Nd and Sr isotope composition of the Guanajuato ankaramite. Decay constants $^{143}Nd/^{144}Nd=0.512638$, $^{147}Sm/^{144}Nd=0.1967$, $^{87}Sr/^{86}Sr=0.7045$, and $^{87}Rb/^{86}Sr = 0.0827$.

Sample	Sm	Nd	$^{147}Sm/^{144}Nd$	$(^{143}Nd/^{144}Nd)i$	ε_{Nd}(T=110 Ma)	Rb	Sr
MA-7	3.89	15.08	0.1569	0.51288	+7.22	5.5	565
	$^{87}Rb/^{86}Sr$		$(^{87}Sr/^{86}Sr)T$	εSr(T=110 Ma)			
	0.02629		0.70355	-11.78			

intruding the base and the top of the Guanajuato Magmatic Sequence, and with basic volcanic rocks with similar undifferentiated character.

Additional evidence supporting contemporaneity between the ankaramite dikes, the magmatic breccias, and the high-magnesian volcanic rocks, is that they are affected by a low-grade metamorphism (prehnite-pumpellyite facies), that is different than greenschist facies affecting the Guanajuato Magmatic Sequence.

The petrological and geochemical constraints suggest that the ankaramite magma was formed:

- By a little-fractionated mantle-derived primary melt (refractory mantle source), without evidence of crustal contamination, consistent with a HFSE-depleted arc-magma source.

- Under hydrous conditions as evidenced by the amphibole occurrence and by a dominant ferromagnesian fractionation.

- By a primitive magma, suggested by high MgO, Cr, and Ni values, and ferromagnesian dominated fractionation.

High MgO lavas (MgO > 9 wt%) ranging in composition from basaltic to low-Si dacite occur in simple and complex arcs of the Circum-Pacific region. The origin of these rocks has been interpreted by hydrous melting of undepleted upper mantle, or subduction-modified mantle in a tectonic environment transitional to rifting. Ankaramitic magmatism is uncommon and typically occurs in deep-fractured or rifted intra-oceanic island-arcs (Beard, 1986), where a tectonic regime of extension and uplift favors that primary, unfractionated high-MgO, Cr and Ni magmas may rise rapidly to the surface retaining their primitive character.

The ankaramitic magmatism of Guanajuato might represent the parental magma of the calc-alkaline and mature tholeiitic magmatic series represented by dioritic to monzodioritic magmatic breccias. Clinopyroxenes and amphiboles similar to those in the ankaramites occur in both the mature tholeiitic and the calc-alkaline magmatic series, both of which also lack orthopyroxene. The salitic trend present in clinopyroxenes of the ankaramitic rocks is similar to that of other island arc basalts and result from concomitant fractionation of Mg-rich minerals and increase of fO_2 in the magma, as a consequence of an increase in water activity in the melts. This Fe-enrichment trend to salitic clinopyroxene is also a function of lower silica activity in the magma, and suggests crystallization of successive assemblages from progressively more hydrous melts (Marcelot et al., 1988). The high water content of the ankaramitic magma is suggested by amphibole occurrence and by the retardation in the crystallization of plagioclase.

Occurrence of ankaramitic dikes in fractures near the base of the arc suggests that an extensional regime has affected the arc crust. Scarcity of this magmatism may reflect a transient regime. Ankaramite dikes of Guanajuato are considered the feeder dikes of MgO (12 wt%), Cr and Ni rich basalts reported at the top of the La Luz tholeiitic sequence (sample HM-90 dated at 108.4± 6.2 m y (±2 sigma); Lapierre et al., 1992), and suggest that undifferentiated magma reached the surface.

These ankaramitic rocks stem from clinopyroxene-saturated primary magmas melting of the mantle source. They provide evidence of primitive magmatic liquid.

The fluids involucrated were derived directly from the subducting slab inducing hydration of the peridotitic mantle wedge.

For the Guanajuato segment, the change from an older tholeiitic to calc-alkaline and mature tholeiitic magmatism is similar to that seen in ancient and modern intra-oceanic island arcs reported in the geological literature.

ACKNOWLEDGEMENTS

I wish to thank Henriette Lapierre and Jean-Louis Zimmermann for performing the chemical and K/Ar analysis. I also thank the reviewers James S. Beard of the Museum of Natural History of Martinsville and Fernando Ortega Gutiérrez of Instituto de Geología for valuable comments which improved the manuscript.

BIBLIOGRAPHIC REFERENCES

Bardsell, M., and Berry, R.F., 1990, Origin and evolution of primitive island arc ankaramites from Western Epi, Vanuatu: Journal of Petrology, v. 31, p. 747-777.

Beard, J.S., 1986, Petrology and tectonic significance of ultramafic to dioritic intrusive complexes in the western Cordillera: Geological Society of America, Abstracts with Programs, v. 18, p. 84.

Campa, M.F. and Coney, P.J., 1983, Tectono-stratigrapic terranes and mineral resource distributions in Mexico: Canadian Journal of Earth Sciences, v. 26, p. 1,040-1,051.

Campa, M.F., 1985, The Mexican Thrust Belt, in Howell, D.G., ed., Tectonostratigraphic terranes of the circum-Pacific region: Houston, Texas, Circum Pacific Council for Energy and Mineral Resource, p. 299-313.

De Paolo, D.J., 1988, Neodymium isotope geochemistry: An introduction: Berlin, Germany, Springer-Verlag, 187 p.

Dick, H.J.B. and Bullen, T., 1986, Chromian spinel as a petrogenetic indicator in abyssal and alpine-type peridotites and spatially associated lavas: Contributions to Mineralogy and Petrology, v. 86, p. 54-76.

Evensen, N.M., Hamilton, P.J., and O'Nions, R.K., 1978, Rare-Earth abondances in chondritic meteorites: Geochimica et Cosmochimica Acta, v. 42, p. 1,199-1,212.

Faure, G., 1977, Principles of isotope geology: New York,, John Wiley & Sons, 464 p.

Foden, J.D., 1983, The petrology of the calcalkaline lavas of Rindaji Volcano, east Sunda Arc—a model for island arc petrogenesis: Journal of Petrology, v. 24, p. 98-130.

Govindaraju, K. and Mevell, G., 1987, Fully automated dissolution and separation methods for inductively coupled plasma atomic emission spectrometry rocks analysis—Application to the determination of Rare Earth Elements: Journal of Analysis Atomic Spectrometry, v. 2, p. 615-621.

Hénoc, J., and Tong, M., 1978, Automatisation de la microsonde: Journal de Microscopie et de Spectroscopie Electroniques, v. 3, p. 247-254.

Lacroix, A., 1916, Compte Rendu Hebdomadaire des Séances de l'Académie des Sciences de Paris, v. 163, p. 177-183.

Lapierre, H., Ortiz-Hernández, Enrique, Abouchami, W., Monod, O., Coulon, Ch., and Zimmermann, J.L.,1992, A crustal section of an intra-oceanic

island arc—The Late Jurassic-Early Cretaceous Guanajuato magmatic sequence, central Mexico: Earth and Planetary Science Letters, v. 108, p. 61-67.

Leake, B.E., 1978, Nomenclature of amphiboles: Mineral Magazine, v. 42, p. 533-563.

Le Maitre, R.W., Bateman, P., Dudek, A., Keller, J., Lameyre, J., Le Bas, M.P., Sabine, P.A., Schmid, R., Sørensen, H., Streckeisen, A., Wolley, A.R. and Zannetin, B., eds., 1989, A classification of igneous rocks and glossary of terms. Recommendations of the International Union of Geological Sciences. Subcommission on the Systematics of the Igneous Rocks: Oxford, U.K., Blackwell Scientific Publications, 193 p.

Marcelot, G., Bardintzeff, J.M., Maury, R.C., and Rançon, J.Ph., 1988, Chemical trends of early-formed clinopyroxene phenocrysts from some alkaline and orogenic basic lavas: Bulletin de la Societé Géologique de France, v. 8, p. 851-859.

Monod, O., Lapierre, H., Chiodi, M., Martínez-Reyes, J., Calvet, Ph., Ortiz-Hernández, Enrique, and Zimmermann, J.L., 1990, Réconstitution d'un arc insulaire intra-océanique au Mexique central: la séquence volcano-plutonique de Guanajuato (Crétacé inférieur): Comptes Rendus de l'Académie des Sciences de Paris, Série II, t. 310, p. 45-51.

Ortiz-Hernández, Enrique, Yta, M., Talavera, O., Lapierre, H., Monod, O., and Tardy, M., 1992, Origine intra-oceánique des formations volcano-plutoniques d'arc du Jurassique supérieur-Crétacé inférieur du Mexique centro-méridional: Comptes Rendus de l'Académie des Sciences de Paris, Série II, t. 312, p. 399-406.

Ortiz-Hernández, L.E., 1998, Mineralogy and geochemistry of Early Cretaceous intra-plate seamounts from Guanajuato, central Mexico: Geofísica Internacional (submitted).

Ortiz-Hernández, L.E., 1998, Aptian-Albian dioritic and monzodioritic magmatic breccias of Guanajuato (Central Mexico)—Implications for the origin of contemporaneous island-arc calc-alkaline and tholeiitic magma series in the Guerrero terrane: Geological Society of America Special Paper (submitted).

Papike, J.J., Cameron, K.L. and Baldwin, K., 1974, Amphiboles and pyroxenes—Characterization of other than quadrilateral components and estimates of ferric iron from microprobe data: Geological Society of America Abstracts with Programs, v. 6, p. 1,053-1,054.

Pearce, J.A., 1983, Role of the sub-continental lithosphere in magma genesis at active continental margins, in C.J. Hawkesworth and M.J. Norry, eds., Continental basalts and mantle xenoliths: Shiva Publishing Nantwich, p. 297-308.

Ramsay, W.R.H., Crawford, A.J., and Foden, J.D., 1984, Field setting, mineralogy, chemistry, and genesis of arc picrites, New Georgia, Salomon Islands: Contributions to Mineralogy and Petrology, v. 88, p. 386-402.

Robinson, P., Spear, F.S., Schumacher, J.C., Laird, J., Klein, , C., Evans, B.W. and Doolan, B.L., 1982, Phase relations of metamorphic amphiboles: Natural ocurrence and theory: Mineralogical Society of America, Reviews in Mineralogy, v. 9B, p. 1-227.

Stein, G., Lapierre, H., Monod, O., Zimmermann, J.L., and Vidal. R., 1994, Petrology of some Mexican Mesozoic-Cenozoic plutons—sources and tectonic environments: South America Journal of Earth Sciences , v. 7, núm. 1, p. 1-7.

Zimmermann, J.L., Vernet, M., Guyetand, G., and Dautel, D., 1985, Données sur potassium et argon (de 1976 a 1984) dans quelques échantillons géochimiques de reférence: Geostandards Newsletter, v. 9, p. 205-208.

Manuscript received: October 5, 1996
Revised manuscript received: October 2, 1998
Manuscript accepted: October 6, 1998